

were uniformly distributed. We find that the outcome doesn't critically depend on the exact magnitude of the length fluctuation as long as it is on the order of microns. In the simulation we use matched polarization between signal and cross talk. Thus the numerical results are the upper bound to the fading margin.

To derive the system margin we calculate the Q-factor.<sup>5</sup> Assuming Gaussian noise statistics and a decision threshold half-way between space and mark,  $BER = 1/2erfc(Q/\sqrt{2})$ , where *erfc* is the complementary error function. This is used to estimate Q from the experimental data and is used in the simulations as well.

Figure 2(a) shows a histogram of experimentally measured  $Q_{dB}$  for  $N = 8$  and  $SXR = 30$  dB, where  $Q_{dB} = 20 \log(Q)$ . Figure 2(b) shows its numerical counterpart. The distribution is one sided with a long tail towards lower  $Q_{dB}$ . The inset of Fig. 2(a) shows BER vs. received power, where 300 points are taken at each received power. Orders of magnitude BER fluctuation occur at nominally identical SXR and received power because of fading. This long tail of the  $Q_{dB}$  distribution is associated with significant system degradation.

Table I summarizes the mean and the standard deviation of the  $Q_{dB}$  distributions. As expected, numerical results consistently predict more severe degradation than experimental data. However the difference is not significant, an observation which justifies our assumption that random polarization skews the system towards worst case. Note that disabling the cross talk paths results in a Gaussian distribution with mean = 15.7 dB and std = 0.07 dB in our measurement system. Thus at high SXR the  $Q_{dB}$

distribution is dominated by other noise in the system. When  $N = 32$ , SXR as high as 55 dB is required.

The effects of coherent cross talk on the system margin have been studied experimentally and numerically. Both approaches show that the Q-factor fluctuates over a long-time scales because of fading. Simulation shows that as much as 55 dB SXR is required for a thirty-two channel system. These results dictate that coherent cross talk be taken into account when one designs lightwave WDM networks.

\*Present Address: MIT, EECS, Office 36-337, Cambridge, Massachusetts 02139

1. E. Goldstein and L. Eskildsen, IEEE Photon. Technol. Lett. 7, 93-94 (1995).
2. P. Legg, D. Hunter, I. Andonovic, P. Barnsley, IEEE Photon. Technol. Lett. 6, 661-663 (1994).
3. E. Goldstein, L. Eskildsen, C. Lin, Y. Silberberg, IEEE Photon. Technol. Lett. 7, 1345-1347 (1995).
4. B. Sklar, IEEE Commun. Mag. 35, 90-109 (1997).
5. N. Bergano, F.W. Kerfoot, C. Davidson, IEEE Photon. Technol. Lett. 5, 304-307 (1993).

**WM31**

**Fast dynamics and power swings in doped-fiber amplifiers fed by highly variable multimedia traffic**

Alberto Bononi, Ljubisa Tančevski,\* Leslie A. Rusch,\*  
*Università di Parma, Dipartimento di Ingegneria dell'Informazione, I-43100 Parma, Italy; E-mail: alberto@tlc.unipr.it*

Erbium-doped fiber amplifier (EDFA) transient gain dynamics in wavelength-division multiplexing (WDM) transmission systems for circuit-switching applications have recently been shown to be rather slow, in the range of tens to hundreds of  $\mu$ s.<sup>1</sup> We show here that such dynamics can be much faster, and give rise to large power swings, in a packet-switching environment with highly variable packet interarrival times, such as with self-similar traffic.<sup>2</sup>

We first examine an EDFA fed by an asynchronous transfer mode (ATM) stream on each wavelength of a WDM system. Fixed-size packets (or cells) have random arrival times, and each wavelength is time-slotted and synchronized at the EDFA input.

The EDFA is fed by eight channels, with ATM cells at 150 Mbit/s (2.82- $\mu$ s cell duration). The EDFA is pumped at 980 nm, with signals at wavelengths 1542-1556 nm, with 2-nm spacing. Input pump power is 18.4 dBm, peak input power per channel is -2 dBm. Cross section values were taken from Ref. 3, Table 4.2, with peak emission  $5.8 \times 10^{-25}$  m<sup>2</sup> and peak absorption  $5.3 \times 10^{-25}$  m<sup>2</sup>. Other EDFA data: fluorescence time 10.5 ms, ion density  $1.14 \times 10^{24}$  m<sup>-3</sup>, overlap factor 0.5, core radius 1.27  $\mu$ m, EDFA length 35 m. Variation in output power, numerically calculated as in Ref. 1, is illustrated in Fig. 1 as channels come on and off. Power swing across the cells is largest when all channels are active, with sub-microsecond transient dynamics. When less input signal power is present, less power swing is observed.

To test the effect of the statistics of packet interarrival times on the power swings, we simulated a 16-channel WDM system, each channel being an independent ON/OFF ATM source. It has been proven that the superposition of many ON/OFF sources whose ON or OFF periods have infinite variance can produce self-similar traffic.<sup>4</sup>

**WM30 Table 1.** Q-factors for Various Number of Cross Talk Paths and SXR Combinations, (a) Mean and Standard Deviation of Experimental Results; (b) Mean and (c) Standard Deviation of Numerical Results

(a)

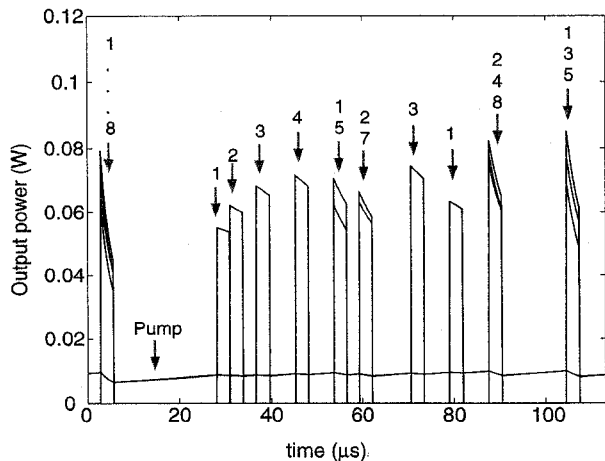
# of Xtalk Path(N)	Mean( $Q_{dB}$ ) for different SXR's(dB)			Std( $Q_{dB}$ ) for different SXR's(dB)		
	30dB	35dB	40dB	30dB	35dB	40dB
2	15.15	15.48	15.70	0.22	0.11	0.08
4	14.99	15.51	15.56	0.34	0.15	0.08
8	14.65	15.22	15.45	0.56	0.26	0.15

(b)

# of Xtalk Path(N)	Mean( $Q_{dB}$ ) for different SXR's(dB)					
	30dB	35dB	40dB	45dB	50dB	55dB
2	15.27	15.42	15.47	15.49		
4	14.96	15.29	15.40	15.46		
8	14.59	15.11	15.34	15.43		
16	13.81	14.79	15.19	15.37	15.45	15.48
32	12.78	14.31	15.00	15.29	15.41	15.46

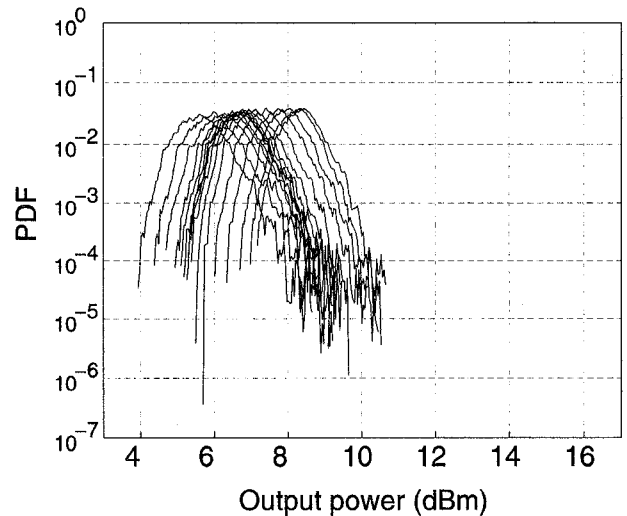
(c)

# of Xtalk Path(N)	Std( $Q_{dB}$ ) for different SXR's(dB)					
	30dB	35dB	40dB	45dB	50dB	55dB
2	0.25	0.07	0.03	0.01		
4	0.47	0.20	0.13	0.06		
8	0.71	0.39	0.17	0.08		
16	1.38	0.69	0.35	0.17	0.07	0.04
32	2.09	1.15	0.51	0.25	0.14	0.07



WM31 Fig. 1. Numerical evaluation of power at output of an EDFA fed by an 8-channel WDM system, with ATM streams at 150 Mbit/s on each channel. -2 dBm/channel input power; active channel number(s) indicated above arrow.

Figure 2(a) shows a histogram of the output power distribution on slots carrying a cell on each channel when the packet input power per channel is -3 dBm, with the 16 channels having 1-nm spacing over the range 1544-1559 nm; remaining parameters are unchanged. The ON times  $T_{on}$  were generated as:  $T_{on} = \lfloor 1/(1-U)^{1/\alpha_{on}} \rfloor$ , where  $U$  is a random variable uniform on  $[0, 1]$ ,  $\lfloor x \rfloor$  indicates the floor function. This implements a (rounded) Pareto distribution, which has infinite variance when  $1 \leq \alpha_{on} \leq 2$ .<sup>2</sup> Here  $\alpha_{on} = 1.2$ , giving a mean (before rounding) equal to



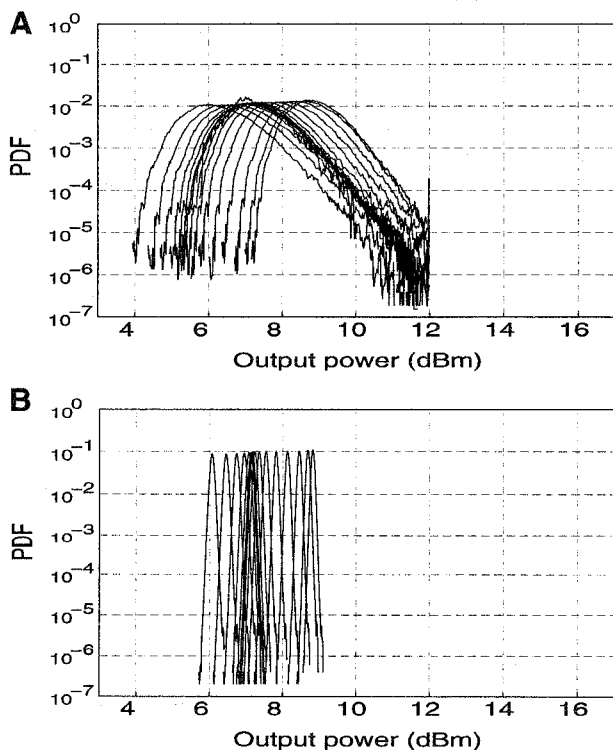
WM31 Fig. 3. Same as Fig. 2, but with ATM cells at 2.5 Gbit/s and  $\alpha_{on} = \alpha_{off} = 1.2$ .

six slots. The OFF periods were generated with  $\alpha_{off} = \alpha_{on}$ . The simulation was run for a million slots, corresponding to 3 s of traffic at 150 Mbit/s. The width of the histogram for each channel at a probability of  $10^{-6}$  is about 7 dBm, constraining the dynamic range of the receiver. Such power spread is due to the long "lulls" during which the EDFA has no power in, and the pump has time to re-invert the erbium ions, thus increasing the gain for the next cell arrival. Figure 2(b) shows similar histograms for the case  $\alpha_{on} = \alpha_{off} = 5$ , for which the ON/OFF times (before rounding) have mean equal to 1.25 and finite variance equal to 0.1. In this finite-variance case the interarrival times have less variability, giving shorter lulls, and thus smaller swings on the cell following the lull.

A similar swing appears even with 2.5-Gbit/s ATM sources, with much shorter cell duration (0.17  $\mu$ s). Figure 3 shows the power histograms, for a simulation of  $10^6$  slot times, at 2.5 Gbit/s, for  $\alpha_{on} = \alpha_{off} = 1.2$ . The histogram width at a probability of  $10^{-6}$  can be extrapolated to about 6 dBm.

\* Université Laval, Département de génie électrique et de génie informatique, Québec, G1K 7P4, Canada

1. Y. Sun, G. Luo, J.L. Zyskind, A.A.M. Saleh, A.K. Srivastava, J.W. Sulhoff, *Electron. Lett.* **32**, 1490-1491 (1996).
2. W. Willinger, M.S. Taqqu, R. Sherman, D.V. Wilson, *IEEE/ACM Trans. Networking* **5**, 71-86 (1997).
3. E. Desurvire, *Erbium-doped fiber amplifiers* (New York, Wiley, 1994).
4. M.S. Taqqu, W. Willinger, R. Sherman, *ACM/SIGCOMM Computer Commun. Rev.* **5-23** (Feb. 1997).



WM31 Fig. 2. Simulated probability density function (PDF) of power at the output of the EDFA, for a 16-channel input WDM system, with ON/OFF ATM sources at 150 Mbit/s with peak input power -3 dBm/channel and Pareto distribution of ON and OFF times, with (top)  $\alpha_{on} = \alpha_{off} = 1.2$  (infinite variance), and (bottom)  $\alpha_{on} = \alpha_{off} = 5$  (finite variance). Leftmost curve: channel at 1544 nm. Rightmost curve: channel at 1559 nm.

WM32

Crosstalk rejection requirements for hybrid WDM system with analog and digital channels

Keang-Po Ho, Shien-Kuei Liaw,\* Department of Information Engineering, The Chinese University of Hong Kong, Shatin, NT, Hong Kong; E-mail: kpho@ie.cuhk.hk

Wavelength-division multiplexed (WDM) systems can utilize the vast bandwidth provided by a single-mode optical fiber. Most WDM